Complete Protection of Nasal and Lung Airways Against SARS-CoV-2 Challenge by Antibody Plus Th1 Dominant N- and S-Specific T-Cell Responses to Subcutaneous Prime and Thermally-Stable Oral Boost Bivalent hAd5 Vaccination in an NHP Study

Elizabeth Gabitzsch[1], Jeffrey T. Safrit[2], Mohit Verma[1], Adrian Rice[1], Peter Sieling[1], Lise Zakin[1], Annie Shin[1], Brett Morimoto[1], Helty Adisetiyo[1], Raymond Wong[1], Ashish Bezawada[2], Kyle Dinkins[1], Joseph Balint[1], Victor Peykov[1], Hermes Garban[1], Philip Liu[1], Pete Bone[3], Andrew Bacon[3], Jeff Drew[3], Daniel C. Sanford[4], Patricia Spilman[1], Lennie Sender[2], Shahrooz Rabizadeh[1], Kayvan Niazi[1], and Patrick Soon-Shiong[1*]

Affiliations

[1]ImmunityBio, LLC, 9920 Jefferson Blvd., Culver City, CA 90232, USA

[2]NantKwest, Inc., 9920 Jefferson Blvd., Culver City, CA 90232, USA

[3]IosBio, Unit 6, Sovereign Business Park, Albert Drive, Burgess Hill, West Sussex, RH159TY, United Kingdom

[4] Battelle Biomedical Research Center, Columbus, Ohio, USA

*Corresponding author: Patrick@Nantworks.com

SHORT TITLE: S plus N vaccine protects NHP from SARS-CoV-2

ONE SENTENCE SUMMARY: hAd5 spike + nucleocapsid SC prime/oral boost vaccine elicits humoral and T-cell responses and protects rhesus macaques from SARS-CoV-2 challenge.

ABSTRACT

We have developed a dual-antigen COVID-19 vaccine incorporating genes for a modified SARS-CoV-2 spike (S-Fusion) protein and the viral nucleocapsid (N) protein with an Enhanced T-cell Stimulation Domain (N-ETSD) with the potential to increase MHC class I/II responses. The adenovirus serotype 5 platform used, hAd5 [E1-, E2b-, E3-], previously demonstrated to be effective in the presence of Ad immunity, can be delivered in an oral formulation that overcomes cold-chain limitations. The hAd5 S-Fusion + N-ETSD vaccine was evaluated in rhesus macaques showing that a subcutaneous prime followed by oral boosts elicited both humoral and Th1 dominant T-cell responses to both S and N that protected the upper and lower respiratory tracts from high titer (1×10^6 $TCID_{50}$) SARS-CoV-2 challenge. Notably, viral replication was inhibited within 24 hours of challenge in both lung and nasal passages, becoming undetectable within 7 days post-challenge.

47 **INTRODUCTION**

48 To address the ongoing COVID-19 pandemic (*1, 2*), particularly in the face of viral evolution
49 and evidence of viral variant resistance to antibodies and convalescent plasma (*3-6*), we have
50 developed a vaccine anticipated to protect individuals from SARS-CoV-2 that has the potential to
51 not only elicit robust humoral responses but also activate T cells. The dual-antigen hAd5 S-Fusion
52 + N-ETSD vaccine (Supplementary Fig. 1) expresses a viral spike (S) protein (S-Fusion) fused to
53 a signal sequence that, as predicted based on reports for similar sequences (*7, 8*), in our *in vitro*
54 studies enhances cell-surface expression of the spike receptor binding domain (S RBD) as
55 compared to S wildtype (Supplementary Fig. 2), the antigen used in the majority of other vaccines
56 being developed. Our vaccine also expresses the viral nucleocapsid (N) protein with an Enhanced
57 T-cell Stimulation Domain (N-ETSD) that directs N to the endo/lysosomal subcellular
58 compartment as demonstrated in Sieling *et al.* (in preprint) (*9*) which is predicted to enhance MHC
59 class II responses (*10-12*).

60 The SARS-CoV-2 vaccine antigens are delivered by an recombinant human adenovirus
61 serotype 5 (hAd5) [E1-, E2b-, E3-] vector platform (Supplementary Fig. 1A) we previously
62 developed to rapidly generate vaccines against multiple agents, allowing production of high
63 numbers of doses in a minimal time frame. The hAd5 platform has unique deletions in the early 1
64 (E1), early 2 (E2b) and early 3 (E3) regions (hAd5 [E1-, E2b-, E3-]), which distinguishes it from
65 other adenoviral vaccine platform technologies under development (*13-15*), and allows it to be
66 effective in the presence of pre-existing adenovirus immunity (*16-19*). We have utilized this
67 platform to produce vaccines against viral antigens such as Influenza, HIV-1 and Lassa fever and
68 have shown induction of both antibodies and cell mediated immunity (*18, 20-23*). In 2009, we
69 showed that vaccination of mice with the hAd5 [E1-, E2b-, E3-] vector expressing H1N1

70 hemagglutinin and neuraminidase genes (*20*) elicited both cell-mediated immunity and humoral
71 responses that protected the animals from lethal virus challenge.

72 The overwhelming majority of other SARS-CoV-2 vaccines in development target only the
73 wildtype S antigen and are expected to elicit SARS-CoV-2 neutralizing antibody responses. In the
74 development of our vaccine, we prioritized the activation T cells to enhance the breath and duration
75 of protective immune responses (*24*); the addition of N in particular was predicted to afford a
76 greater opportunity for T cell responses (*25-27*). T cells may provide immune protection at least
77 as important as the generation of antibodies. In a study of SARS-CoV-2 convalescent patients,
78 virus-specific T cells were seen in most patients, including asymptomatic individuals, even those
79 with undetectable antibody responses (*27*).

80 In our preliminary studies of the hAd5 S-Fusion + N-ETSD vaccine in a murine model, we
81 saw that the vaccine not only elicits T helper cell 1 (Th1)-dominant antibody responses to both S
82 and N, it activates T-cells (Supplementary Fig. 3). We then looked the potential of the hAd5 S-
83 Fusion + N-ETSD vaccine to re-capitulate T-cell activation prompted by natural SARS-CoV-2
84 infection (*9*). To do this, we transduced monocyte-derived dendritic cells (MoDCs) from SARS-
85 CoV-2 convalescent individuals with the dual-antigen vaccine, incubated the S-Fusion and N-
86 ETSD-expressing MoDCs with T cells from those same individuals, and saw that the vaccine
87 antigens induce interferon-γ (IFN-γ) secretion by both CD4+ and CD8+ T cells (9). This
88 demonstrates that T cells from SARS-CoV-2 convalescent individuals 'recall' the S-Fusion and
89 N-ETSD antigens presented by transduced MoDCs as if they were re-exposed to the virus itself.
90 This T-cell recall of vaccine antigens suggests that, conversely, hAd5 S-Fusion + N-ETSD
91 vaccination will generate T cells that will recognize SARS-CoV-2 antigens upon viral infection
92 and protect the vaccinated individual from disease.

93 The generation of T-cell responses may be a critical feature for a vaccine to be efficacious
94 against the many variants whose emergence, at least in part, may be an escape response to
95 antibodies generated by either first wave virus (*28*) or, as suggested in Wang *et al.* (in preprint)
96 (*29*) by antibody-based vaccines. As further reported in Wang *et al.*, neutralization by 14 of 17 of
97 the most potent mRNA vaccine-elicited monoclonal antibodies (mAbs) was either decreased or
98 abolished variants E484K, N501Y or the K417N:E484K:N501Y combination (*6, 30*). They also
99 found these variants were selected for when recombinant vesicular stomatitis virus (rVSV)/SARS-
100 CoV-2 S was cultured in the presence of these mAbs, which is highly suggestive that the presence
101 of these antibodies act as an evolutionary force driving the appearance of new variants. T cells are
102 not vulnerable to such forces and, if effectively established by vaccination, may provide protection
103 (*31-33*) against existing viral strains and escape mutants.
104 We hypothesized that vaccination with the hAd5 S-Fusion + N-ETSD vaccine, which
105 generates both neutralizing antibodies and memory T cells, would be protective in the rhesus
106 macaque and that room temperature oral formulations would be effective as boosts.
107 In the next step in development of the hAd5 S-Fusion + N-ETSD vaccine, we formulated
108 GMP (Good Manufacturing Practice)-grade liquid and oral forms of the vaccine for testing in non-
109 human primates (NHP). A key objective of the NHP study design was to assess the efficacy of a
110 subcutaneous (SC) prime followed by a thermally-stable (*34*) oral boost.
111 An oral boost provides several advantages in SARS-CoV-2 vaccination, including a greater
112 potential for generating mucosal immunity particularly in the gastrointestinal tract (*35*) one of the
113 major sites of infection (*36*). SARS-CoV-2 is a mucosal virus and is only rarely detected in blood
114 (*37, 38*), therefore vaccines that specifically target mucosal immunity are of interest (*39*).
115 Compelling additional advantages of a thermally-stable oral boost are that it would likely

116 transform the global distribution of vaccines, especially in developing nations and potentially
117 enable patients to self-administer the boost(s) at home. Because the hAd5 S-Fusion + N-ETSD
118 construct induces both humoral and CMI responses to both antigens, it also has the potential to
119 serve as a 'universal' heterologous booster vaccine to the multitude of SARS-CoV-2 vaccines
120 under development.

121 Here, we report our findings from our study designed to determine the efficacy of the hAd5
122 S-Fusion + N-ETSD vaccine in rhesus macaques when delivered as either an SC prime with SC
123 and oral boosts (SC-SC-Oral; n =5) or as an SC prime and two oral boosts (SC-Oral-Oral; n = 5)
124 both using a regimen of prime on Day 0 and boosts on Days 14 and 28 to maximize T cell
125 responses. Design details are presented in *Materials and Methods* and Supplementary Fig. S4**.** The
126 goals of the study were to assess the immunogenicity of a dual-antigen hAd5 vaccine in both SC
127 and oral formulations, and the potential of oral dose to serve as a boost following a single SC
128 prime. Most importantly, we sought to assess cell-mediated T-cell response and protection of nasal
129 passages and lung from SARS-CoV-2 infection after challenge as well as the rate of viral
130 clearance.

131 ***Clinical signs, hematology and clinical chemistry***

132 No clinical signs were noted during the twice daily observations for clinical signs of toxicity
133 due to vaccination and no animals died during the two weeks after one subcutaneous immunization
134 of 1x 10^{11} vaccine particles (VP) or a week after an oral booster of 1x10^{10} IU of hAd5-S-Fusion+N-
135 ETSD. In addition, no gross pathological effects or adverse events were observed and there were
136 no notable changes in body weight (Supplementary Fig. 5). Lastly, hematology and clinical
137 chemistry revealed no abnormalities as a result of vaccination (Supplementary Tables 1 and 2).
138

139 **An SC prime with oral boosts elicits generation of neutralizing, anti-spike antibodies**

140 As shown in Figure 1, all SC-Oral-Oral vaccinated NHP produced anti-S IgG that increased
141 after both the Day 14 and Day 28 oral boosts (Fig. 1A and B). Sera from 4 of 5 SC-Oral-Oral NHP,
142 taken at baseline and every week starting at Day 14 and up to Day 42, demonstrated inhibition in
143 the neutralization assay (Fig. 1C) that assesses the inhibition of binding of S RBD to recombinant
144 angiotensin-converting enzyme 2 (ACE2) and is reported to correlate with the ability of sera to
145 neutralize the SARS-CoV-2 virus (*40*).

146 Anti-S IgG production was similar for SC-SC-Oral (where the first boost was SC) hAd5 S-
147 Fusion + N-ETSD vaccinated NHP (Fig. 1D and E) and sera from all five NHP in this group
148 demonstrated inhibition in the surrogate assay for viral neutralization (Fig. 1F).

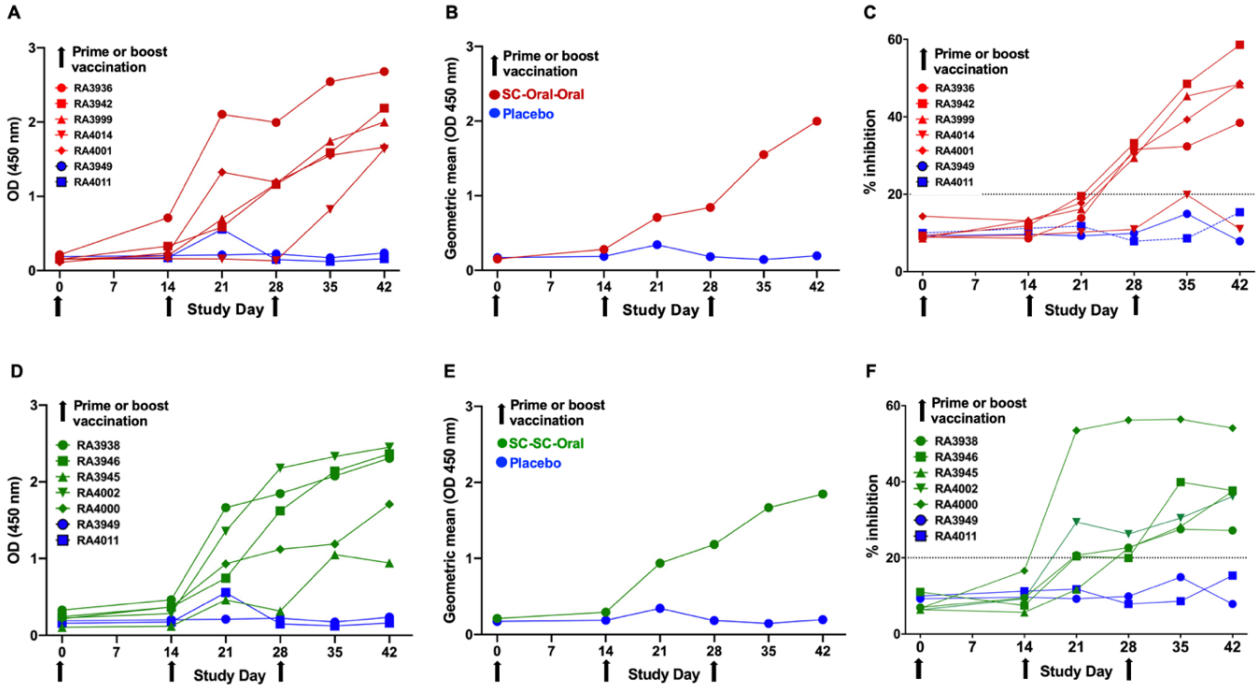

149
150 **Fig. 1** *Humoral responses and neutralizing capability of sera from hAd5 S-Fusion + N-ETSD*
151 *vaccinated NHP*. Anti-spike IgG levels (ELISA; OD 450nm) are shown for (A) individual SC-
152 Oral-Oral NHP along with the (B) geometric mean and (C) inhibition in the surrogate assay. These
153 data are also shown for SC-SC-Oral NHP: (D) individual anti-S IgG, (E) geometric mean, and (F)
154 inhibition in the surrogate assay. Inhibition above 20% (dashed line) with a sera dilution of 1:30
155 is correlated with neutralization of SARS-CoV-2 infection. NHP received vaccination on Days 0,
156 14 and 28 (black arrows).
157

158 **SC prime, oral boost vaccination reduces viral load in nasal passages and lung after SARS-**
159 **CoV-2 challenge**

160 RT-qPCR analysis of genomic RNA (gRNA) was performed on nasal swab and
161 bronchoalveolar lavage (BAL) samples to determine the amount of virus present. SC-Oral-Oral
162 vaccination of NHP reduced SARS-CoV-2 gRNA in the nasal swab samples as compared to
163 placebo control NHP from Day 57, the first day after challenge (Fig. 2A and B; Supplementary
164 Table 3). Viral gRNA in this group continued to diminish to levels that were very low or below
165 the level of detection (LOD) in all vaccinated animals by Day 63, 7 days after challenge. Placebo
166 controls had moderate to high levels (range 2E+09 – 8.4E+03 gene copies/mL) of SARS-CoV-2
167 present in nasal swab samples for the duration of the study.

168 In the lungs (bronchoalveolar lavage, BAL) of SC-Oral-Oral NHP, gRNA also decreased
169 rapidly, with the geometric mean showing a ~2 log decrease in vaccinated NHP compared to
170 placebo NHP at Day 57, just one day after challenge (Fig. 2C and D, Supplementary Table 4).

171 In the group receiving an SC and oral boost (SC-SC-Oral), SARS-CoV-2 gRNA in nasal swab
172 samples was also reduced similarly to that seen in SC-Oral-Oral vaccinated primates, with viral
173 gRNA decreasing to levels that were very low or below the LOD in all vaccinated animals by Day
174 63 (Fig. 2E and F; Supplementary Table 3). In the lungs of SC-SC-Oral NHP, gRNA also showed
175 a ~2 log decrease on Day 57 (Fig. 2G and H; Supplementary Table 4**).**

176

177

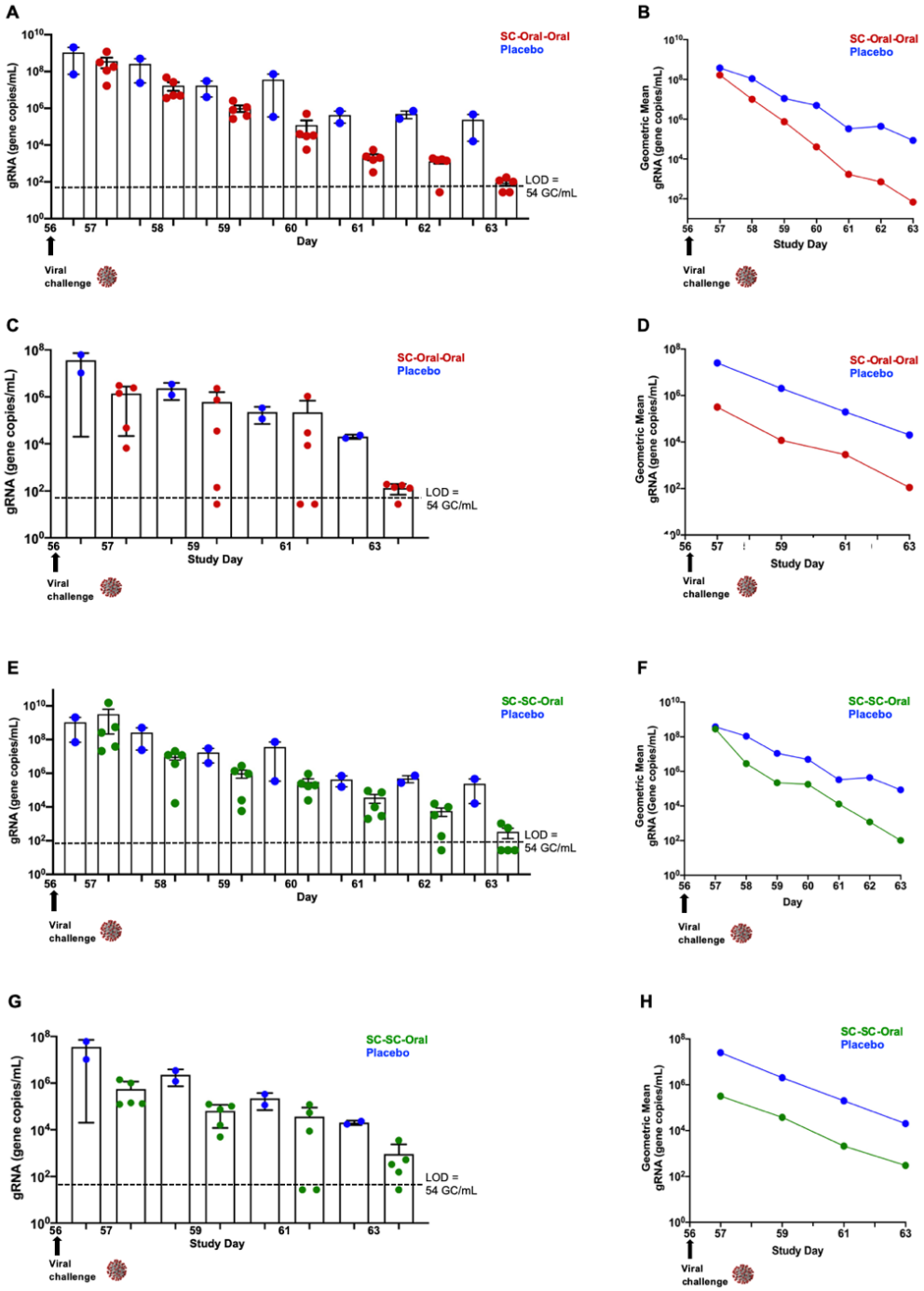

Fig. 2 *Viral load (gRNA) in nasal passages and lung of SC-Oral-Oral and SC-SC-Oral vaccinated NHP post-challenge.* (A) Individual viral gRNA (RT qPCR) and (B) the geometric mean for nasal swab samples; and (C) gRNA and (D) the geometric mean for bronchoalveolar lavage (BAL) samples from SC-Oral-Oral NHP. (E) Individual gRNA and (F) the geometric mean for nasal swab samples; and (G) gRNA and (H) the geometric means for BAL samples from SC-SC-Oral NHP. SARS-CoV-2 challenge was on Day 56 (black arrows). The level of detection (LOD; dashed line) was 54 gene copies/mL (GC/mL) for gRNA and 119 GC/mL for sgRNA. For values below the LOD, half the LOD value (or 27 GC/mL for gRNA and 59 GC/mL for sgRNA) was used for graphing of individual values and calculation of the geometric mean.

188 **SC prime, oral boost vaccination immediately inhibited viral replication in nasal passages**
189 **and lung after SARS-CoV-2 challenge**

190 The presence of replicating virus in nasal swab samples was determined by RT qPCR of
191 subgenomic RNA (sgRNA). By Day 60, 4 days post-challenge, sgRNA was below the LOD for
192 two SC-Oral-Oral primates and, starting on Day 61, below the LOD for all primates that received
193 only oral boosts (Figure 3A and B and Supplementary Table 5).

194 In the lungs of SC-Oral-Oral NHP, sgRNA also decreased as compared to placebo starting at
195 Day 57, and was below the LOD in all by Day 63 (Fig. 3C and D, Supplementary Table 6).

196 Evidence of replicating viruses in nasal passages also decreased rapidly in SC-SC-Oral NHP
197 and was below the LOD by Day 59 in two primates and in all primates by Day 63 (Fig. 3E and F;
198 Supplementary Table 5); and in the lungs of this group, sgRNA decreased by ~2 logs compared to
199 placebo control on Day 57, one day after challenge, with sgRNA being below the LOD at Day 63
200 in 4 of 5 primates, and just above the LOD in the 5th (Fig. 3 G and H; Supplementary Table 6).

201 Not only was there a rapid decrease of both viral load and replicating viruses in nasal passages
202 and lung, it is notable that there was no growth of viruses following challenge. This implies the
203 presence of pre-existing humoral and cellular immunity resulting in rapid clearance of the virus
204 upon infection.

205

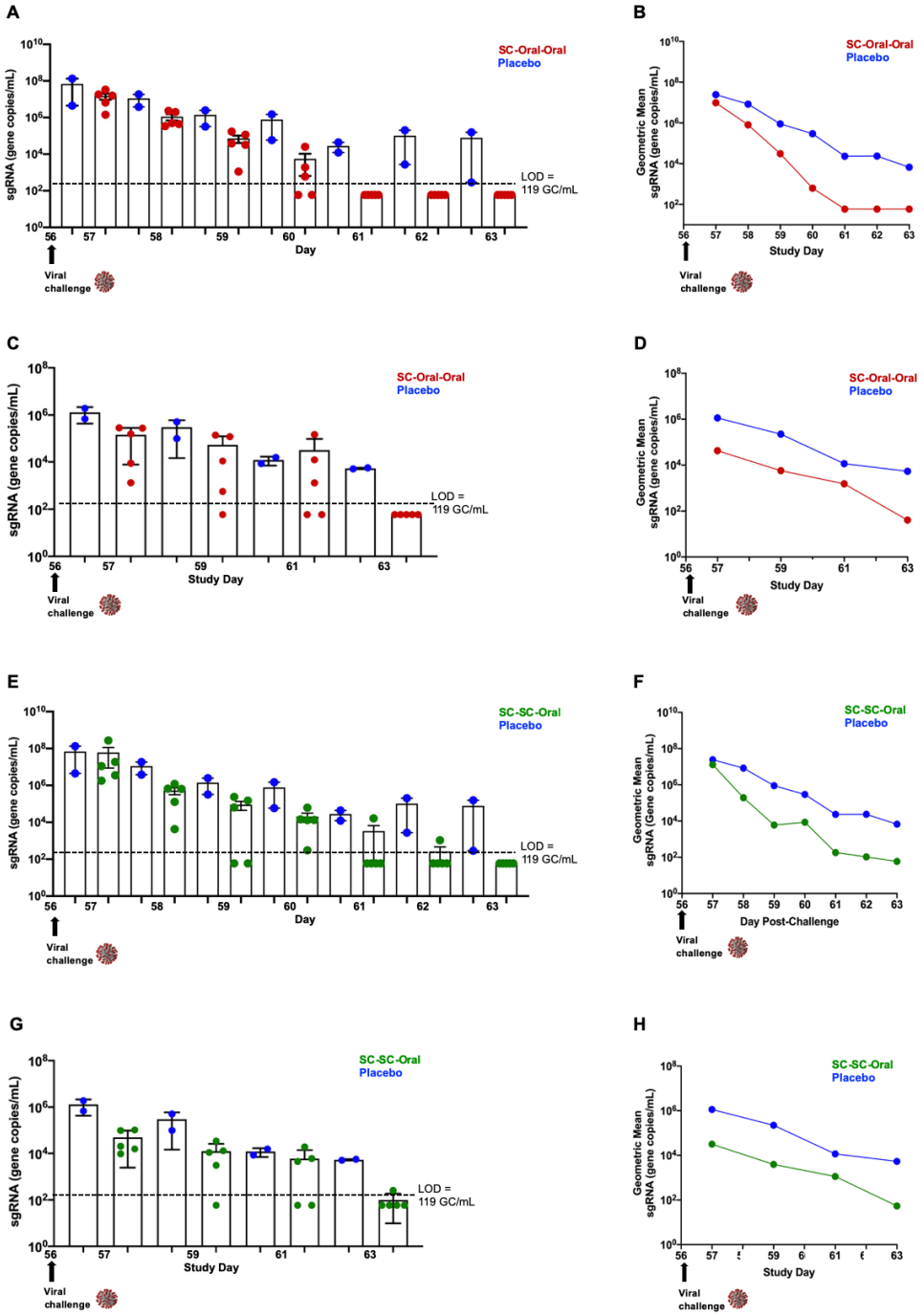

Fig. 3 *Viral replication (sgRNA) in nasal passages and lung in SC-Oral-Oral and SC-SC-Oral vaccinated NHP post-challenge.* (A) Individual viral sgRNA (RT qPCR) and (B) the geometric mean for nasal swab samples; and (C) sgRNA and (D) the geometric mean for bronchoalveolar lavage (BAL) samples from SC-Oral-Oral NHP. (E) Individual sgRNA and (F) the geometric mean for nasal swab samples; and (G) sgRNA and (H) the geometric means for BAL samples from SC-SC-Oral NHP. SARS-CoV-2 challenge was on Day 56 (black arrows). The level of detection (LOD; dashed line) was 54 gene copies/mL (GC/mL) for gRNA and 119 GC/mL for sgRNA. For values below the LOD, half the LOD value (or 27 GC/mL for gRNA and 59 GC/mL for sgRNA) was used for graphing of individual values and calculation of the geometric mean.

216 **Immediate protection of NHP from SARS-Cov-2 challenge may be due to the presence of T**
217 **cells responsive to both S and N, and rapid viral clearance to activation of memory B cells**

218 Peripheral blood mononuclear cell (PBMC)-derived T-cell responses to the antigens delivered
219 by the hAd5 S-Fusion + N+ETSD vaccine, spike and nucleocapsid, were determined by ELISpot
220 on Day 0 before prime vaccination, on Day 14 (before boost) and on Day 35, one week after the
221 second Day 28 boost. T cells from SC-Oral-Oral vaccinated primates secreted interferon-gamma
222 (IFN-γ) in response to both S and N peptides on Days 14 and 35 (Fig. 4A). Interleukin-4 (IL-4)
223 secretion was very low (Fig. 4B), indicating the T-cell responses were T helper cell 1 (Th1)
224 dominant, as reflected by the IFN-g/IL-4 ratio (Fig. 4C).

225 For sera collected in the post-challenge period, a microneutralization assay (see Methods) was
226 used to assess SARS-CoV-2 neutralization capability as reflected by the 'MN50', that is, the serum
227 dilution that correlates to a 50% reduction in viral infectivity as compared to a no-serum control.
228 A rapid increase in neutralization capability of sera for NHP receiving only oral boosts was seen
229 over the two weeks following challenge (Fig. 4D) that mirrored decreases in nasal gRNA and
230 sgRNA (Fig. 4E and F, respectively) and lung gRNA and sgRNA (Fig. 4G and H, respectively).
231 Notably, sera from placebo group primates did not show an increase in neutralizing capability after
232 challenge (Fig. 4D and L), suggesting the existence of memory B cells in the vaccinated group and
233 the absence of such cells in the unvaccinated placebo group. Further studies are needed to confirm
234 this hypothesis.

235 For SC-SC-Oral vaccinated NHP, findings were very similar for reactive T cells during the
236 pre-challenge vaccination period (Fig. 4I-K) and for neutralization capability in the post-challenge
237 period (Fig. 4L), including the mirroring of decreasing gRNA and sgRNA in nasal passages and
238 lung (Fig. 4M-P).

239 We hypothesize that the presence of cytotoxic T cells due to vaccination (Fig. 4A-C and I-K)
240 led to the almost immediate decrease in viral replication within the first 24 hours post-challenge
241 (Fig. 4F, H, N, and P), and the continued decreases over the following two weeks that mirrored
242 increases in neutralization capability of sera from vaccinated, but not placebo, NHP reflect the
243 contribution of anti-S-producing memory B cells (Fig. 4D and L).

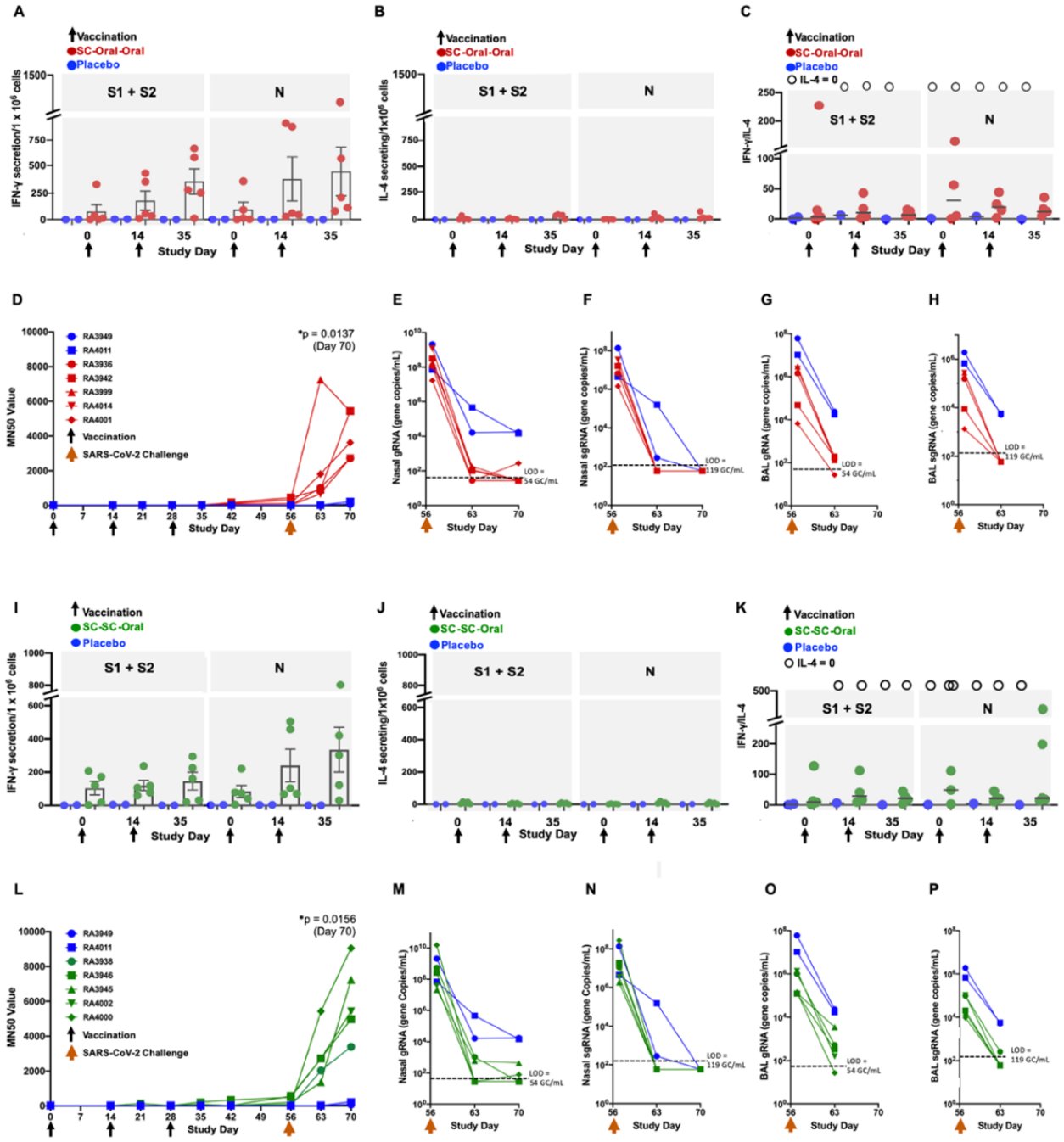

244

245 **Fig. 4** *T-cell responses to vaccination and neutralization capability of sera post-SARS-CoV-2*
246 *challenge*. (A) Interferon-γ (IFN-γ) and (B) interleukin-4 (IL-4) secretion by PBMC-derived T
247 cells from SC-Oral-Oral vaccinated NHP in response to spike (S) and nucleocapsid (N) peptides
248 as determined by ELISpot as well as (C) the ratio IFN-γ/IL-4 ratio are shown. Ratios of 'infinity'
249 due to undetectable IL-4 are represented as open circles. Cells pulsed with PMA-ionomycin were
250 used as positive controls as described in *Methods* (not presented). Data graphed with mean and
251 SEM. (D) MN50 (dilution factor which SARS-CoV-2 infection of Vero E6 cells is inhibited by
252 50%) throughout the course of the study is shown; an unpaired, two-tailed Student's t-test was
253 used to compare MN50s for vaccinated and placebo NHP on Day 70. Nasal gRNA (E) and sgRNA
254 (F) on Days 57, 63 and 70, as well as lung gRNA (G) and sgRNA on Days 57 and 63 are presented.
255 The same data are shown for SC-SC-Oral NHP, including T-cell responses (I-J), MN50 (L), nasal
256 gRNA (M) and sgRNA (N), as well as lung gRNA (O) and sgRNA (P). The level of detection for
257 gRNA was 54 gene copies/mL (GC/mL) and for sgRNA was 119 GC/mL. Half the LOD was used
258 for graphing of data below the LOD.
259
260 This study demonstrates that in the rhesus macaque NHP model, subcutaneous prime and oral
261 boost dual-antigen hAd5 S-Fusion + N-ETSD vaccination protects both nasal and lung airways
262 against SARS-CoV-2 challenge. The inhibition of viral replication in nasal passages as evidenced
263 by decreased sgRNA on the first day after viral challenge was notable, as was continuous clearance
264 of virus to levels below detection within 7 days of challenge in all (10/10) animals (Figs. 2 and 3);
265 and, while the rhesus macaque is not a model for the assessment of transmission, these rapid
266 reductions in nasal viral replication are encouraging and support the investigation of the ability of
267 this vaccine to prevent transmission in future studies.
268 The ability of hAd5 S-Fusion + N-ETSD vaccination to elicit virus-neutralizing anti-S
269 antibodies (Fig. 1) and T cells responsive to both S and N (Fig. 3) - particularly when viewed with
270 the rapid increase in the neutralization capability of sera post-challenge that is likely indicative of
271 the presence of memory B cells - suggests the vaccine establishes broad immunity against severe
272 SARS-CoV-2 infection.
273 The potential of the hAd5 S-Fusion + N-ETSD SC prime, oral boost vaccine to generate
274 cytotoxic T cells is, in our opinion, a key feature, given the critical role of T cells play in protection

275 from infection in COVID-19 convalescent patients where SARS-CoV-2 specific T cells were
276 identified even in the absence of antibody responses (*27*).

277 The apparent nearly immediate reduction of viral replication by the hAd5 S-Fusion + N-ETSD
278 vaccination is in contrast to the reported findings for other adenovirus-vectored S-only vaccine
279 NHP studies (*13, 14*), wherein there was evidence of continued viral replication in some animals
280 for at least a day after challenge. Even when challenged with the relatively high titer of 1 $x10^6$
281 $TCID_{50}$/mL as compared to titers used in some other NHP vaccine studies (*13, 41*), vaccinated
282 animals in our study appeared to be protected from the earliest time point assessed. This rapid
283 protection and clearance was particularly evident in the lung, where both viral load and viral
284 replication were ~1-2 logs lower than placebo in both vaccinated groups just one day after
285 challenge.

286 The protection conferred by hAd5 S-Fusion + N-ETSD vaccination of NHPs by SC and oral
287 boost administration particularly reveal the potential for this vaccine to be developed for world-
288 wide distribution, especially in light of the escape variants resistant to antibodies and convalescent
289 plasma, now rapidly spreading throughout the world (*5, 6*). The oral hAd5 S-Fusion + N-ETSD
290 formulation would not require ultra-cold refrigeration like many COVID vaccines currently in
291 development. Dependence on the cold-chain for distribution to geographically remote or under-
292 developed areas causes shipping and storage challenges and will likely reduce the accessibility of
293 the RNA-based COVID-19 vaccines.

294 Our thermally-stable oral hAd5 S-Fusion + N-ETSD vaccine, due its expression of S and N,
295 also has the potential to act as a 'universal' boost to other previously administered vaccines that
296 deliver only S antigens. This use would also be facilitated by cold-chain independence and
297 warrants further exploration.

298 The hAd5 S-Fusion + N-ETSD vaccine delivered as an SC prime and boost is in Phase 1
299 clinical trials and the thermally-stable oral vaccine has entered Phase 1 trials as both a prime and
300 boost, and as a boost to an SC prime.
301

302 **ACKNOWLEDGEMENTS**

303 We would like to thank the following members of the Battelle group for their contributions
304 in the execution of this study; Chris Cirimotich, Katie Albanese, Phyllis Herr-Calomeni, Bradley
305 Brown, Sara Pfeifer, Carrie Fetzek, Ashley Hay, Andy Puttmann, Amy Allen, and Kevin Coty.
306 We thank Phil Yang of ImmunityBio for his ongoing coordination of project reports for this study.
307 We would also like to thank the DHHS, NIH/NIAID and ASPR/BARDA for funding the study.
308

309 **REFERENCES**

310 1. J. T. Wu, K. Leung, G. M. Leung, Nowcasting and forecasting the potential domestic and
311 international spread of the 2019-nCoV outbreak originating in Wuhan, China: a
312 modelling study. *The Lancet* **395**, 689-697 (2020).
313 2. R. Li *et al.*, Substantial undocumented infection facilitates the rapid dissemination of
314 novel coronavirus (SARS-CoV-2). *Science* **368**, 489-493 (2020).
315 3. Y. Weisblum *et al.*, Escape from neutralizing antibodies by SARS-CoV-2 spike protein
316 variants. *Elife* **9**, e61312 (2020).
317 4. Q. Li *et al.*, The Impact of Mutations in SARS-CoV-2 Spike on Viral Infectivity and
318 Antigenicity. *Cell* **182**, 1284-1294.e1289 (2020).
319 5. S. Cele *et al.*, Escape of SARS-CoV-2 501Y.V2 variants from neutralization by
320 convalescent plasma. *medRxiv*, 2021.2001.2026.21250224 (2021).
321 6. H. Tegally *et al.*, Emergence and rapid spread of a new severe acute respiratory
322 syndrome-related coronavirus 2 (SARS-CoV-2) lineage with multiple spike mutations in
323 South Africa. *medRxiv*, 2020.2012.2021.20248640 (2020).
324 7. Y. Kou *et al.*, Tissue plasminogen activator (tPA) signal sequence enhances
325 immunogenicity of MVA-based vaccine against tuberculosis. *Immunology letters* **190**,
326 51-57 (2017).
327 8. J.-Y. Wang *et al.*, Improved expression of secretory and trimeric proteins in mammalian
328 cells via the introduction of a new trimer motif and a mutant of the tPA signal sequence.
329 *Applied Microbiology and Biotechnology* **91**, 731-740 (2011).

330 9. P. Sieling *et al.*, Th1 Dominant Nucleocapsid and Spike Antigen-Specific CD4+ and CD8+
331 Memory T Cell Recall Induced by hAd5 S-Fusion + N-ETSD Infection of Autologous
332 Dendritic Cells from Patients Previously Infected with SARS-CoV-2. *medRxiv*,
333 2020.2011.2004.20225417 (2020).
334 10. K. R. Niazi *et al.*, Activation of human CD4+ T cells by targeting MHC class II epitopes to
335 endosomal compartments using human CD1 tail sequences. *Immunology* **122**, 522-531
336 (2007).
337 11. K. Y. Lin *et al.*, Treatment of established tumors with a novel vaccine that enhances
338 major histocompatibility class II presentation of tumor antigen. *Cancer research* **56**, 21-
339 26 (1996).
340 12. T. C. Wu *et al.*, Engineering an intracellular pathway for major histocompatibility
341 complex class II presentation of antigens. *Proceedings of the National Academy of*
342 *Sciences of the United States of America* **92**, 11671-11675 (1995).
343 13. N. B. Mercado *et al.*, Single-shot Ad26 vaccine protects against SARS-CoV-2 in rhesus
344 macaques. *Nature* **586**, 583-588 (2020).
345 14. N. van Doremalen *et al.*, ChAdOx1 nCoV-19 vaccine prevents SARS-CoV-2 pneumonia in
346 rhesus macaques. *Nature* **586**, 578-582 (2020).
347 15. A. Amalfitano *et al.*, Production and Characterization of Improved Adenovirus Vectors
348 with the E1, E2b, and E3 Genes Deleted. *Journal of virology* **72**, 926 (1998).
349 16. M. E. Gatti-Mays *et al.*, A Phase I Trial Using a Multitargeted Recombinant Adenovirus 5
350 (CEA/MUC1/Brachyury)-Based Immunotherapy Vaccine Regimen in Patients with
351 Advanced Cancer. *Oncologist* **25**, 479 (2019).
352 17. J. P. Balint *et al.*, Extended evaluation of a phase 1/2 trial on dosing, safety,
353 immunogenicity, and overall survival after immunizations with an advanced-generation
354 Ad5 [E1-, E2b-]-CEA(6D) vaccine in late-stage colorectal cancer. *Cancer immunology,*
355 *immunotherapy : CII* **64**, 977-987 (2015).
356 18. E. S. Gabitzsch *et al.*, Novel Adenovirus type 5 vaccine platform induces cellular
357 immunity against HIV-1 Gag, Pol, Nef despite the presence of Ad5 immunity. *Vaccine* **27**,
358 6394-6398 (2009).
359 19. M. A. Morse *et al.*, Novel adenoviral vector induces T-cell responses despite anti-
360 adenoviral neutralizing antibodies in colorectal cancer patients. *Cancer Immunology,*
361 *Immunotherapy* **62**, 1293-1301 (2013).
362 20. F. R. Jones *et al.*, Prevention of influenza virus shedding and protection from lethal H1N1
363 challenge using a consensus 2009 H1N1 HA and NA adenovirus vector vaccine. *Vaccine*
364 **29**, 7020-7026 (2011).
365 21. E. S. Gabitzsch *et al.*, A preliminary and comparative evaluation of a novel Ad5 [E1-, E2b-
366] recombinant-based vaccine used to induce cell mediated immune responses.
367 *Immunology letters* **122**, 44-51 (2009).
368 22. E. S. Gabitzsch *et al.*, Induction and comparison of SIV immunity in Ad5 naïve and Ad5
369 immune non-human primates using an Ad5 [E1-, E2b-] based vaccine. *Vaccine* **29**, 8101-
370 8107 (2011).
371 23. J. Maruyama *et al.*, Adenoviral vector-based vaccine is fully protective against lethal
372 Lassa fever challenge in Hartley guinea pigs. *Vaccine* **37**, 6824-6831 (2019).
373 24. S. C. Gilbert, T-cell-inducing vaccines - what's the future. *Immunology* **135**, 19-26 (2012).

374 25. N. Le Bert *et al.*, SARS-CoV-2-specific T cell immunity in cases of COVID-19 and SARS, and
375 uninfected controls. *Nature* **584**, 457 (2020).
376 26. A. Grifoni *et al.*, Targets of T Cell Responses to SARS-CoV-2 Coronavirus in Humans with
377 COVID-19 Disease and Unexposed Individuals. *Cell* **181**, 1489 (2020).
378 27. T. Sekine *et al.*, Robust T cell immunity in convalescent individuals with asymptomatic or
379 mild COVID-19. *Cell* **183**, 158 (2020).
380 28. A. J. Greaney *et al.*, Complete Mapping of Mutations to the SARS-CoV-2 Spike Receptor-
381 Binding Domain that Escape Antibody Recognition. *Cell Host Microbe*, S1931-
382 3128(1920)30624-30627 (2020).
383 29. Z. Wang *et al.*, mRNA vaccine-elicited antibodies to SARS-CoV-2 and circulating variants.
384 *bioRxiv*, 2021.2001.2015.426911 (2021).
385 30. J. Zahradník *et al.*, SARS-CoV-2 RBD in vitro evolution follows contagious mutation
386 spread, yet generates an able infection inhibitor. *bioRxiv*, 2021.2001.2006.425392
387 (2021).
388 31. M. Hellerstein, What are the roles of antibodies versus a durable, high quality T-cell
389 response in protective immunity against SARS-CoV-2? *Vaccine: X* **6**, 100076 (2020).
390 32. R. Channappanavar, C. Fett, J. Zhao, D. K. Meyerholz, S. Perlman, Virus-specific memory
391 CD8 T cells provide substantial protection from lethal severe acute respiratory syndrome
392 coronavirus infection. *Journal of virology* **88**, 11034-11044 (2014).
393 33. K. McMahan *et al.*, Correlates of protection against SARS-CoV-2 in rhesus macaques.
394 *Nature* **10.1038/s41586-020-03041-6**, (2020).
395 34. M. Stewart, S. J. Ward, J. Drew, Use of adenovirus as a model system to illustrate a
396 simple method using standard equipment and inexpensive excipients to remove live
397 virus dependence on the cold-chain. *Vaccine* **32**, 2931-2938 (2014).
398 35. J. Holmgren, C. Czerkinsky, Mucosal immunity and vaccines. *Nature Medicine* **11**, S45-
399 S53 (2005).
400 36. F. Xiao *et al.*, Evidence for Gastrointestinal Infection of SARS-CoV-2. *Gastroenterology*
401 **158**, 1831-1833.e1833 (2020).
402 37. O. Gallo, L. G. Locatello, A. Mazzoni, L. Novelli, F. Annunziato, The central role of the
403 nasal microenvironment in the transmission, modulation, and clinical progression of
404 SARS-CoV-2 infection. *Mucosal Immunol*, 1-12 (2020).
405 38. H. Q. Yu *et al.*, Distinct features of SARS-CoV-2-specific IgA response in COVID-19
406 patients. *Eur Respir J* **56**, 2001526 (2020).
407 39. L. Moreno-Fierros, I. García-Silva, S. Rosales-Mendoza, Development of SARS-CoV-2
408 vaccines: should we focus on mucosal immunity? *Expert Opinion on Biological Therapy*
409 **20**, 831-836 (2020).
410 40. C. W. Tan *et al.*, A SARS-CoV-2 surrogate virus neutralization test based on antibody-
411 mediated blockage of ACE2-spike protein-protein interaction. *Nat Biotechnol* **38**, 1073-
412 1078 (2020).
413 41. L. Feng *et al.*, An adenovirus-vectored COVID-19 vaccine confers protection from SARS-
414 COV-2 challenge in rhesus macaques. *Nature communications* **11**, 4207 (2020).
415 42. A. C. Walls *et al.*, Structure, Function, and Antigenicity of the SARS-CoV-2 Spike
416 Glycoprotein. *Cell* **181**, 281-292.e286 (2020).

417 43. W. Zeng *et al.*, Biochemical characterization of SARS-CoV-2 nucleocapsid protein.
418 *Biochemical and biophysical research communications*, S0006-0291X(0020)30876-30877
419 (2020).
420 44. S. Srinivasan *et al.*, Structural Genomics of SARS-CoV-2 Indicates Evolutionary Conserved
421 Functional Regions of Viral Proteins. *Viruses* **12**, 360 (2020).
422 45. V. K. Shah, P. Firmal, A. Alam, D. Ganguly, S. Chattopadhyay, Overview of Immune
423 Response During SARS-CoV-2 Infection: Lessons From the Past. *Front Immunol* **11**, 1949
424 (2020).
425 46. A. Sattler *et al.*, SARS–CoV-2–specific T cell responses and correlations with COVID-19
426 patient predisposition. *The Journal of Clinical Investigation* **130**, 6477-6489 (2020).
427 47. J. Schaack *et al.*, Promoter strength in adenovirus transducing vectors: down-regulation
428 of the adenovirus E1A promoter in 293 cells facilitates vector construction. *Virology* **291**,
429 101-109 (2001).
430 48. G. W. Wilkinson, A. Akrigg, Constitutive and enhanced expression from the CMV major
431 IE promoter in a defective adenovirus vector. *Nucleic Acids Res* **20**, 2233-2239 (1992).
432 49. C. W. Tan *et al.*, A SARS-CoV-2 surrogate virus neutralization test based on antibody-
433 mediated blockage of ACE2-spike protein-protein interaction. *Nat Biotechnol* **38**, 1973
434 (2020).
435 50. R. Wölfel *et al.*, Virological assessment of hospitalized patients with COVID-2019. *Nature*
436 **581**, 465-469 (2020).
437 51. M. A. Hamilton, R. C. Russo, R. V. Thurston, Trimmed Spearman-Karber method for
438 estimating median lethal concentrations in toxicity bioassays. *Environmental Science &*
439 *Technology* **11**, 714-719 (1977).
440
441
442
443
444
445
446
447
448
449
450
451

452 # Supplementary Materials

453 **Materials and Methods**
454
455 *The hAd5 S-Fusion + N-ETSD vaccine*
456 To generate the hAd5 S-Fusion + N-ETSD vaccine we utilized the hAd5 [E1-, E2b-, E3-]
457 platform (Fig. S1A) into which a wildtype spike (S) (Fig. S1B) sequence [accession number
458 YP009724390] modified with a proprietary linker peptide sequence was cloned and as well as
459 wildtype nucleocapsid (N) (Fig, S1B) sequence [accession number YP009724397] with a
460 proprietary Enhanced T-cell Stimulation Domain (ETSD) signal sequence to direct translated N to
461 the endosomal/lysosomal pathway. The SARS-CoV-2 S protein is found on the viral surface and
462 its receptor binding domain (RBD) interacts with the host angiotensin-converting enzyme 2
463 (ACE2) and gains entry to the host cell to initiate infection (*42*). Antibodies against the S RBD are
464 neutralizing, preventing this first step in infection.
465
466 The nucleocapsid protein is found in the interior of the virus and is highly conserved and
467 antigenic (*43, 44*). it also plays an important role in T-cell responses (*45, 46*).
468
469 The powerful cytomegalovirus (CMV) promoter (*47, 48*) drives expression in the hAd5
470 construct. The hAd5 S-Fusion + N-ETSD vaccine construct is shown below in Supplementary Fig.
471 S1.
472

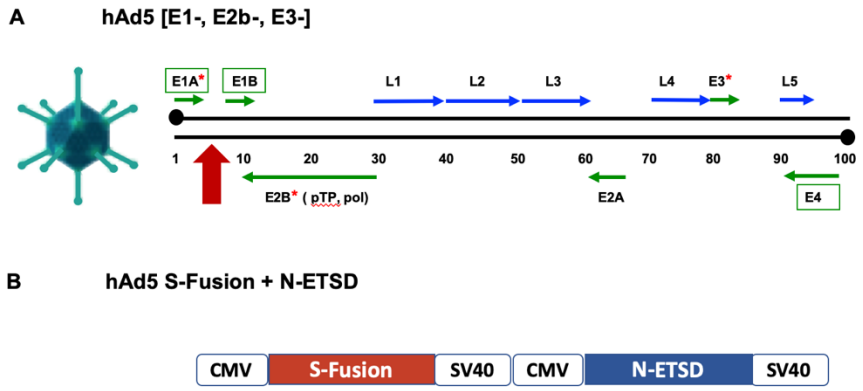

473
474
475 **Fig. S1** *The hAd5 platform and the hAd5 S-Fusion + N-ETSD construct.* (A) The human
476 adenovirus serotype 5 vaccine platform with E1, E2b, and E3 regions deleted (*) is shown. The
477 vaccine construct is inserted in the E1 regions (red arrow). (B) The dual-antigen vaccine comprises
478 both S-Fusion and N-ETSD under control of cytomegalovirus (CMV) promoters and with C-
479 terminal SV40 poly-A sequences delivered by the hAd5 [E1-, E2b-, E3-] platform.
480
481 *Transduction of HEK-293T cells and flow cytometry*
482 Relative levels of cell-surface expression of S RBD after transduction of human embryonic
483 kidney (HEK) 293T cells with various S-expressing hAd5 vaccines was determined by flow
484 cytometry. HEK 293T cells (2.5 x 10^5 cells/well in 24 well plates) were grown in DMEM
485 containing 10% FBS and PSA (100 units/mL penicillin, 100 µg/mL streptomycin, 0.25 µg/mL
486 Amphotericin B) at 37°C. Cells were either untransduced or transduced with hAd5 S-WT, S-

487 Fusion, or S-Fusion + N-ETSD viral particles at a multiplicity of infection (MOI) of 10. For
488 detection of spike on Days 1, 2, 3 and 7 after infection, cells were transferred by gently pipetting
489 into medium and labeled with an anti-RBD monoclonal antibody (clone D003 Sino Biological)
490 and F(ab')2-Goat anti-Human IgG-Fc secondary antibody conjugated with R-phycoerythrin
491 (Thermofisher). Labeled cells were acquired using a Thermo-Fisher Attune NxT flow cytometer
492 and analyzed using Flowjo Software. Results are shown in Supplementary Figure S2.
493
494 **The Mouse Study**
495
496 *Vaccination of CD-1 mice*
497 CD-1 female mice (Charles River Laboratories) 7 weeks of age were used for immunological
498 studies performed at the vivarium facilities of Omeros Inc. (Seattle, WA). After an initial blood
499 draw, mice were injected with either hAd5 spike wildtype (S-WT) (n = 3) or vaccine candidate
500 hAd5 S-Fusion + N-ETSD (n = 8) on Day 0 at a subcutaneous (SC) dose of 1 x10^{10} viral particles
501 (VP). Mice received a second SC vaccine dose on Day 21 and on Day 28, blood was collected *via*
502 the submandibular vein from isoflurane-anesthetized mice for isolation of sera and then mice were
503 euthanized for collection of spleen and other tissues.
504
505 *ELISpot assay for assessment of cytokine secretion by T cells*
506 ELISpot assays were used to detect cytokines secreted by splenocytes from inoculated mice.
507 Fresh splenocytes were used on the same day, as were cryopreserved splenocytes containing
508 lymphocytes. The cells (2-4 x 10^5 cells per well of a 96-well plate) were added to the ELISpot
509 plate containing an immobilized primary containing an immobilized primary antibody to either
510 IFN-γ (BD catalogue # 512525) or IL-4 (BD catalogue # 511819), and were pulsed with 2 μg/ml
511 of SARS-CoV-2 S or N peptide pools (JPT Peptide Technologies catalogue # PM-WCPV-S-1 and
512 PM-WCPV-NCAP-1 respectively). Negative and positive controls were cells cultured with media
513 alone or Concanavalin A (ConA, 0.46 μg/ml), respectively. After aspiration and washing to
514 remove cells and media, cytokine secretion was detected by biotinylated antibodies to either IFN-
515 γ (BD catalogue # 551818) or IL-4 (BD catalogue # 551804), followed by labeling with a
516 secondary streptavidin/horseradish peroxidase conjugate (BD catalogue # 557630). Spot
517 development was completed using a peroxidase substrate kit (Vector Labs catalogue # SK-4200).
518 The number of spots per well (2-4 x 10^5 PBMCs) was counted using an ELISpot plate reader.
519 Numbers for graphing were adjusted to spot-forming cells per 10^6 PBMCs.
520
521 *ELISA for detection of antibodies in the mouse study*
522 For antibody detection in sera from inoculated mice, ELISAs specific for spike and
523 nucleocapsid antibodies, as well as for IgG subtype (IgG1, IgG2a, IgG2b, and IgG3) antibodies
524 were used. A microtiter plate was coated overnight with 100 ng of either purified recombinant
525 SARS-CoV-2 S-FTD (full-length S with fibritin trimerization domain, constructed and purified
526 in-house by ImmunityBio), SARS-CoV-2 S RBD (Sino Biological, Beijing, China; Cat # 401591-
527 V08B1-100) or purified recombinant SARS-CoV-2 nucleocapsid (N) protein (Sino Biological,
528 Beijing, China; Cat # 40588-V08B) in 100 μL of coating buffer (0.05 M Carbonate Buffer, pH
529 9.6). The wells were washed three times with 250 μL PBS containing 1% Tween 20 (PBST) to
530 remove unbound protein and the plate was blocked for 60 minutes at room temperature with 250
531 μL PBST. After blocking, the wells were washed with PBST, 100 μL of diluted serum samples
532 were added to wells, and samples incubated for 60 minutes at room temperature. After incubation,

533 the wells were washed with PBST and 100 µL of a 1/5000 dilution of anti-mouse IgG HRP (GE
534 Health Care; Cat # NA9310V), or anti-mouse IgG_1 HRP (Sigma; Cat # SAB3701171), or anti-
535 mouse IgG_{2a} HRP (Sigma; Cat # SAB3701178), or anti-mouse IgG_{2b} HRP (Sigma; catalog#
536 SAB3701185), or anti-mouse IgG_3 HRP conjugated antibody (Sigma; Cat # SAB3701192) was
537 added to wells. For positive controls, a 100 µL of a 1/5000 dilution of rabbit anti-N IgG Ab or 100
538 µL of a 1/25 dilution of mouse anti-S serum (from mice immunized with purified S antigen in
539 adjuvant) were added to appropriate wells. After incubation at room temperature for 1 hour, the
540 wells were washed with PBS-T and incubated with 200 µL o-phenylenediamine-dihydrochloride
541 (OPD substrate (Thermo Scientific Cat # A34006) until appropriate color development. The color
542 reaction was stopped with addition of 50 µL 10% phosphoric acid solution (Fisher Cat # A260-
543 500) in water and the absorbance at 490 nm was determined using a microplate reader (SoftMax®
544 Pro, Molecular Devices).
545
546 *Calculation of relative µg amounts of antibodies*
547 A standard curve of IgG was generated and absorbance values were converted into mass
548 equivalents for both anti-S and anti-N antibodies. Using these values, we were able to calculate
549 that hAd5 S-Fusion + N-ETSD vaccination generated a geometric mean value of 5.8 µg S-specific
550 IgG and 42 µg N-specific IgG per milliliter of serum.
551
552 The analysis of antibodies and subtypes, and ELISpot for IFN-γ and IL-4 secretion ratios are shown
553 in Supplementary Figure S3.
554
555 **The NHP study**
556
557 The study, performed at Battelle Biomedical Research Center (Columbus, Ohio), was
558 sponsored by the Biomedical Advanced Research & Development Authority (BARDA), Office of
559 the Assistant Secretary for Preparedness and Response (ASPR), Department of Health and Human
560 Services (DHHS) and the National Institutes of Health/National Institute for Allergy and Infectious
561 Diseases (NIH/NIAID) (Washington, DC). Battelle is a Public Health Service (PHS) Animal
562 Welfare Assurance approved facility. The study protocol was approved by the Institutional Animal
563 Care and Use Committee (ACUC). All aspects of the animal study protocol were designed to
564 minimize stress in the animals.
565
566 *Dosing and sample collection*
567 A total of 12 naïve rhesus macaques weighing >/= 2.5 Kg and being >2.5 years of age were
568 used in the study. All rhesus macaques were tested and confirmed negative within 45 days of
569 receipt for Mycobacterium tuberculosis, simian immunodeficiency virus (SIV), simian T-
570 lymphotropic virus-I (STLV-1), simian retroviruses 1 and 2 (SRV-1 and SRV-2) via PCR,
571 Macacine herpesvirus I (Herpes B virus), and Trypanosoma cruzi (ELISA and PCR).
572 We compared two SC injections administered in the center of the back just caudal to the
573 scapular region of 1 x 10^{11} vaccine particles (VP) of hAd5 S-Fusion + N-ETSD on Days 0 and 14
574 followed by an oral capsule 1x 10^{10} infectious units (IU) of hAd5 S-Fusion + N-ETSD delivered
575 via a feeding tube after a minimum of 4 hours of fasting on Day 28 (SC-SC-Oral, Group 1) to one
576 prime SC injection and two oral boost doses with the same dosages and timing (SC-Oral-Oral,
577 Group 2), as shown in Supplementary Figure S4.

578 Vaccination Group 1 (SC-SC-Oral comprised 3 male and 2 female, Group 2 (SC-Oral-Oral)
579 2 male and 3 female, and Group 3 (placebo) 1 male and 1 female randomized NHP.
580 On Day 42, NHPs were transferred to a BSL-3 facility and on Day 56 they were challenged
581 via the intratracheal (0.5 mL) and intranasal (0.25 mL per nares) routes with a total dose of
582 approximately 1 x10^6 $TCID_{50}$ SARS-CoV-2 strain USA-WA1/2020. Nasal and oropharyngeal
583 swabs were collected daily from Day 56 (prior to challenge) through Day 63 (7 days post-
584 challenge) and again on Day 70 (14 days post-challenge). In addition, bronchoalveolar lavages
585 (BALs) were performed on Days 57, 59, 61, and 63.

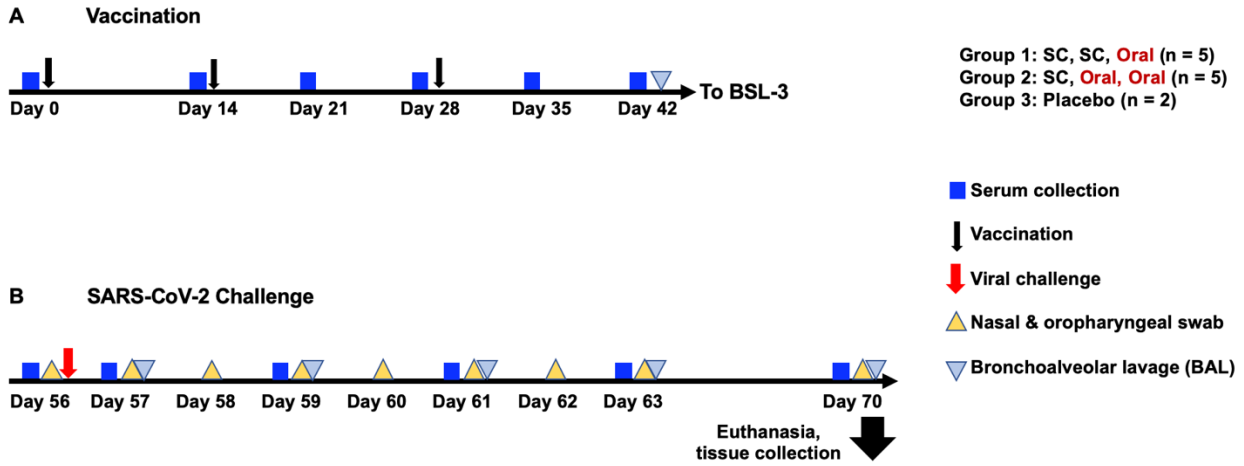

586
587 **Fig. S4** *NHP study design*. Group 1 NHP (n = 5) were vaccinated by subcutaneous (SC) injection
588 of 1 x 10^{11} VP hAd5 S-Fusion + N-ETSD on Days 0 and 14, and received an oral boost of 1 x 10^{10}
589 IU hAd5 S-Fusion + N-ETSD on Day 28. Group 2 NHP (n = 5) were vaccinated similarly, but
590 both boosts were oral. Sera were collected as indicated (blue box) throughout the study. On Day
591 42, NHP were transferred to a BSL-3 facility for viral challenge (red arrow) with 1x10^6 $TCID_{50}$
592 VP of SARS-CoV-2 intranasally and intratracheally. Nasal and oropharyngeal samples (yellow
593 triangles) and bronchoalveolar lavage (BAL) samples (gray triangles) were collected as indicated.
594 Animals were euthanized on Day 70 and tissues collected for pathological analyses.
595
596 *Clinical signs*
597 NHP in all groups were observed twice daily from study Day -7 until the end of the study on
598 Day 70 for clinical signs, including but not limited to anorexia (weights were taken), hunched
599 posture, lethargy, respiratory distress, activity (recumbent, weak, or unresponsive), convulsions,
600 and other abnormal clinical observations. Blood was collected from a femoral artery or vein,
601 saphenous vein, or appropriate vessel of anesthetized animals at baseline, and Days 14, 21, 28, 35,
602 42, 56 (challenge Day), 57, 59, 61, 63, and 70 (End Study). Collected blood was used for clinical
603 chemistry and hematological analyses as well as isolation of PBMCs. Body weights are shown in
604 Supplementary Figure S5, hematology in Table S1 and clinical chemistry in Table S2.
605
606 *Statistical analysis*
607 For comparison of animals in groups, One-Way ANOVA was used with an appropriate post-
608 hoc analysis (for example, Tukey's or Dunnett's) for specific comparisons. For head-to-head
609 analyses, a two-tailed unpaired Student's T-test was used. For all statistical analyses, *p <= 0.05,
610 **p < 0.01, ***p<0.001, and ****p<0.0001. All statistical analysis was performed using
611 GraphPad Prism 9 software.
612

613 *ELISA for anti-Spike IgG*

614 IgG against recombinant spike protein in NHP sera or plasma was determined using an
615 Enzyme-Linked ImmunoSorbent Assay (ELISA) wherein 96 well EIA/RIA plates (ThermoFisher,
616 Cat# 07-200-642) were coated with 50 µL/well by a 1 µg/mL solution of purified recombinant
617 SARS-CoV-2-derived Spike protein (S-Fusion; ImmunityBio, Inc.) suspended in coating buffer
618 (0.05 M carbonate-bicarbonate, pH 9.6) and incubated overnight at 4°C. Plates were washed three
619 times with 150 µL of TPBS solution (PBS + 0.05%Tween 20) then 100 µL/well of blocking
620 solution (2% non-fat milk in TPBS) was added and incubated for 1 hour at room temperature (RT).
621 Plasma and serum samples were heat-inactivated at 56°C for 1 hour before use and 1:50 dilutions
622 were prepared in 1% non-fat milk in TPBS. Plates were washed as described above and 50 µL/well
623 of each dilution was added to the plate and incubated at RT for 1 hour. Plates were washed three
624 times with 200 µL of TPBS before addition of 50µL/well of a 1:6000 dilution of HRP-conjugated,
625 cross-absorbed goat anti-monkey IgG (H+L) secondary antibody (ThermoFisher, Cat# PA1-
626 84631) in 1% non-fat milk/TPBS and incubation for 1 hour at RT.

627 Plates were then washed three times with 200 µL of TPBS and 50 µL of 3,3',5,5'-
628 tetramethylbenzidine (TMB) substrate (VWR, Cat# 100359-156) was added to each well and
629 incubated at RT for 10 minutes. The reaction was stopped by addition of 50 µL/well of 1N sulfuric
630 acid (H_2SO_4). The optical density (OD) at 450 nm was measured using a Synergy 2 plate reader
631 (BioTek Instruments, Inc) and data is analyzed using Prism 8 (GraphPad Software, LLC).

632

633 *cPass™ surrogate assay for determination of the presence of neutralizing antibodies*

634 The presence of neutralizing, anti-spike antibodies in sera from all NHP was determined by
635 assay of sera collected on Days 0, 14, 21, 28, 35 and 42 using the surrogate virus neutralization
636 assay, cPass™ (*49*). The assay is based on assessment of inhibition of binding of the spike receptor
637 binding domain (RBD) to its human host receptor (in the assay, recombinant) angiotensin
638 converting enzyme 2 (ACE2), with inhibition above 20% being correlated with a level of anti-S
639 antibody that is predicted to be neutralizing. All sera samples were diluted 1:30.

640

641 *ELISpot for assessment of cytokine secretion*

642 ELISpot assays were used to detect cytokines secreted by fresh peripheral blood mononuclear
643 cells (PBMCs) isolated from the blood of NHP study animals. PBMCs were isolated from whole
644 blood by standard density gradient centrifugation and frozen in liquid nitrogen until use. PBMCs
645 were thawed and re-suspended in RPMI 10% human AB serum, then pulsed with 2 µg/ml of
646 SARS-CoV-2 S or N peptide pools (JPT Peptide Technologies catalogue # PM-WCPV-S and PM-
647 WCPV-NCAP-1 respectively). Negative and positive controls were cells cultured with media
648 alone or phorbol myristate acetate (PMA, 50 ng/ml) and ionomycin (1 µg/ml), respectively. For
649 IFN-γ assessment, PBMCs were cultured (17 hours at 37°C) in a microtiter plate (Millipore
650 catalogue # MAIPS4510) containing an immobilized primary antibody to capture NHP-specific
651 IFN-γ (MabTech catalogue # 3421M-3-1000). IFN-γ was detected by a secondary antibody to
652 human IFN-γ conjugated to biotin (MabTech catalogue # 3420-6-250). A streptavidin/horseradish
653 peroxidase conjugate (Thermo Fisher catalogue # 21126) was used detect the biotin-conjugated
654 secondary antibody. IFN-γ spot development was completed using a peroxidase substrate kit
655 (Vector Labs catalogue # SK-4200). The number of spots per well (3.5×10^5 PBMCs) was counted
656 using an ELISpot plate reader. IL-4 was assessed using a commercial ELISpot kit (MabTech
657 catalogue # 3410-APW-2) using the manufacturer's instructions. Numbers for graphing were
658 adjusted to spot-forming cells per 10^6 PBMCs.

659 *Determination of viral load and viral replication post-challenge*
660 RT-qPCR assays were performed to quantify total SARS-CoV-2 RNA copies including
661 genomic RNA using the nucleocapsid protein gene as a target or subgenomic RNA copies that are
662 replication intermediates of the virus using the envelope protein (E) gene as a target. These assays
663 were performed to quantify viral loads following SARS-CoV-2 challenge. RNA was isolated from
664 swabs and bronchioalveolar lavage fluid using the Indispin QIAcube HT Pathogen Kit (Indical
665 Bioscience, Germany) on the QIAcube HT instrument (Qiagen, Germany). The isolated RNA was
666 then evaluated in RT-qPCR using the TaqMan Fast Virus 1-step Master Mix (Thermo Fisher
667 Scientific) on a QuantStudio Flex 6 Real-Time PCR System (Applied Biosystems; Foster City,
668 CA). The primers and probe for total SARS-CoV-2 RNA quantitation were specific to the
669 nucleocapsid protein gene, corresponding to the N1 sequences from the Centers for Disease
670 Control and Prevention (CDC) 2019-Novel Coronavirus (2019-nCoV) Real-Time RT-PCR
671 Diagnostic Panel (https://www.cdc.gov/coronavirus/2019-ncov/lab/rt-pcr-panel-primer-
672 probes.html) except that the probe quencher was modified to Non-Fluorescent Quencher-Minor
673 Groove Binder (NFQ-MGB) (Thermo Fisher Scientific). The primers and probe for the
674 subgenomic RNA quantitation were specific to the E gene subgenomic RNA (Integrated DNA
675 Technologies, Iowa) (*50*). A standard curve comprised of synthetic RNA containing the
676 corresponding target sequence from SARS-CoV-2 isolate WA1 sequence (GenBank Accession
677 Number MN985325.1) (Bio-Synthesis, Inc.; Lewisville, TX) was included on each PCR plate for
678 absolute quantitation of SARS-CoV-2 RNA copies in each sample. Thermocycling conditions
679 were: Stage 1 - 50°C for 5 min for one cycle; Stage 2 - 95°C for 20 sec for one cycle; Stage 3 -
680 95°C for 3 sec and 60°C for 30 sec for 40 cycles. Data analysis was performed using the
681 QuantStudio 6 software-generated values (total copies per well of each sample) and additional
682 calculations to determine SARS-CoV-2 RNA or subgenomic RNA copies per mL of fluid.
683
684 *Microneutralization assay (MNA)*
685 The neutralizing antibody titer in hAd5 S-Fusion + N-ETSD vaccinated and placebo NHP sera
686 were measured using a Plaque Reduction Neutralization Test (PRNT) carried out in the BSL-4. In
687 brief, the serum samples were heat-inactivated at 56 °C for 90 min, serially diluted two-fold, and
688 pre-incubated with virus stock at 37 °C for 1 hour. The virus/serum mixture was added to 90-100%
689 confluent monolayer Vero E6 cells (BEI, Cat. No. NR-596) in 96-well plates and incubated for 2
690 days at 37ºC with 5% CO_2. The virus-containing medium was then replaced with 80% acetone for
691 cell fixation. Plates were incubated with an anti-nucleocapsid protein primary antibody cocktail
692 (clones HM1056 and HM1057; EastCoast Bio, North Berwick, ME) for 60 minutes at 37°C. The
693 plates were washed and the secondary antibody (goat anti-mouse IgG Horse Radish Peroxidase
694 (HRP) conjugate; Fitzgerald, North Acton, MA) was added to the wells and the plates were
695 incubated for 60 minutes at 37°C (Battelle Memorial Institute, Patent Number 63/041,551
696 Pending, 2020). After the plates were washed, the substrate was added and the plates were
697 incubated at 37°C. Stop solution was added and the plates were read for optical density at 405 nm
698 wavelength. Neutralizing activity is defined as at least 50% reduction in signal from the virus only
699 (VC) wells relative to cells control (CC) wells following the formula [(average VC –average
700 CC)/2] + average CC. The median neutralizing titer (MN50) was calculated using Spearman-
701 Kärber analysis method (*51*).
702
703
704

705 **Supplementary Results**
706
707 *Surface expression of spike receptor binding domain (RBDS) in hAd5 S-wildtype (W), hAd5 S-*
708 *Fusion, or hAd5 S-Fusion + N-ETSD transduced HEK-293T cells*
709
710 Cell surface expression of S RBD was enhanced with hAd5 S-Fusion compared to hAd5 S-WT,
711 and the dual-antigen hAd5 S-Fusion + N-ETSD construct further enhanced cell surface expression
712 in transduced HEK-293T cells, as shown in Fig. S2.
713

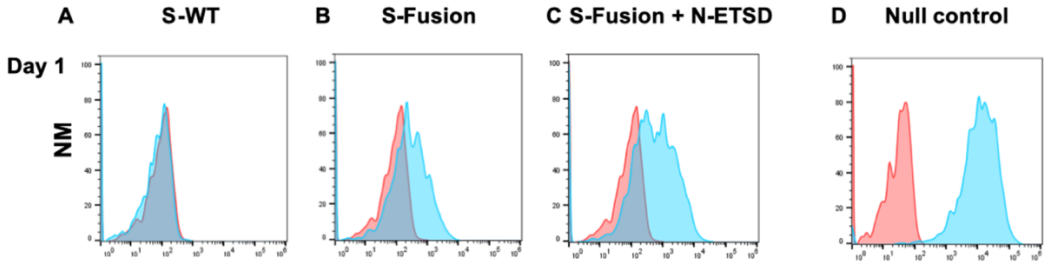

714
715 **Fig. S2** *S RBD cell-surface display is enhanced by S-Fusion and S-Fusion + N-ETSD.* Cell surface
716 expression of S RBD after transduction of human embryonic kidney (HEK)-293T cells as detected
717 by flow cytometry (normalized to mode, NM) using an anti-RBD antibody with (A) hAd5 S-
718 wildtype (S-WT), (B) hAd5 S-Fusion, (C) hAd5 S-Fusion + N-ETSD, or (D) hAd5 Null control
719 reveals increased surface expression of S RBD by S-Fusion that is further enhanced in S-Fusion +
720 N-ETSD. Untransduced (pink) and transduced (blue).
721
722 *hAd5 S-Fusion + N-ETSD vaccination of CD-1 mice elicits Th1 helper cell dominant antibody and*
723 *T-cell responses*
724
725 CD-1 mice vaccinated with the hAd5 S-Fusion + N-ETSD construct produced significantly higher
726 anti-S IgG than mice receiving hAd5 S-WT (Fig. S3A).
727

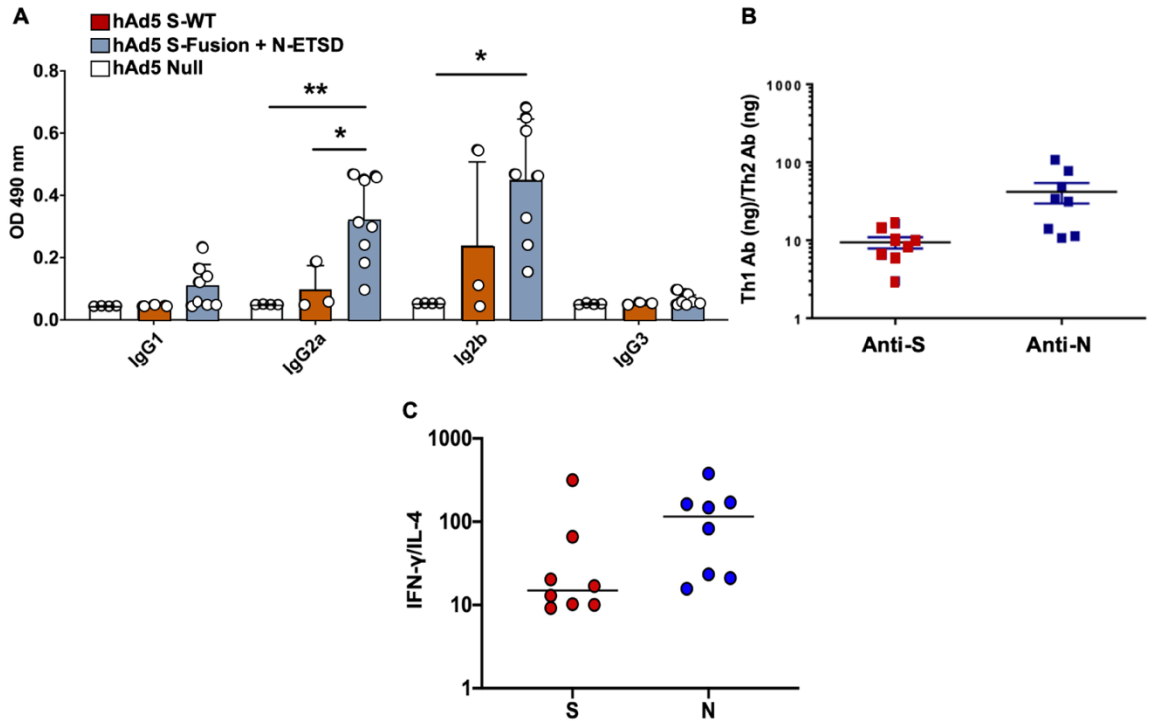

Fig. S3. *Anti-S IgG and Th1 dominance in hAd5 S-Fusion + N-ETSD vaccinated mice.* (A) hAd5 S-Fusion + N-ETSD vaccinated mice produced significantly higher levels of IgG2a and IgG2b anti-S antibodies as compared to mice vaccinated with hAd5 S-WT. Statistical analysis performed using One-way ANOVA and Tukey's post-hoc comparison of groups. (B) In mice, both anti-S and anti-nucleocapsid (N) antibody responses were Th1 dominant, as were (C) T-cell responses (based on the ELISpot IFN-γ/IL-4 ratio) to both the S and N peptide pools.

The NHP Study

Clinical signs

No clinical signs were noted during the twice daily observations for clinical signs of toxicity due to vaccination and no animals died during the two weeks after one subcutaneous immunization of 1x 10^{11} VP or a week after an oral booster of 1x10^{10} IU of hAd5-S-Fusion+N-ETSD. No gross pathological effect or adverse events were observed and there were no notable changes in body weight (Supplementary Fig. S5).

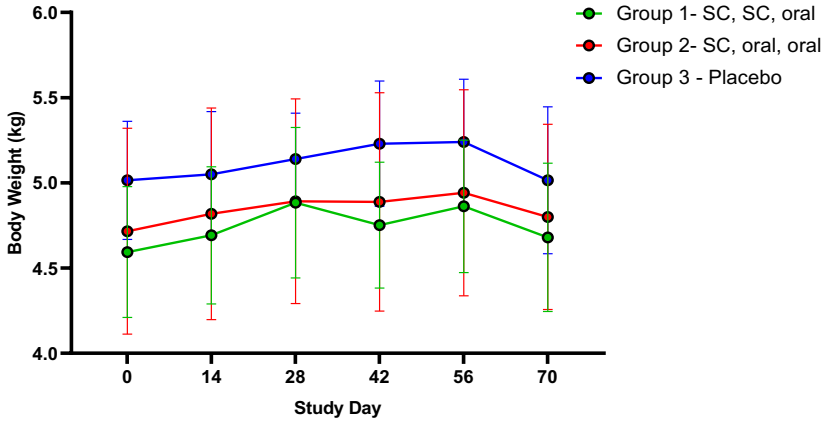

Figure S5. *NHP body weights over the course of the study*. Body weights are shown in Kg; note y-axis range is 4-6 Kg.

Hematology

Hematological parameters evaluated in Group 1 and 2 hAd5 S-Fusion + N-ETSD and Group 3 placebo control animals are presented in Table S1**.** Only hemoglobin was consistently slightly lower in Group 2 NHP as compared to Group 3 placebo for all post-vaccination time points.

Table S1. *Hematological parameters in hAd5 S-Fusion + N-ETSD vaccinated Group 1 and Group 2 NHP versus placebo Group 3*.

Study Day	Day 0			Day 14			Day 28			Day 42			Day 56			Day 63			Day 70		
Parameter	**G1**	**G2**	**G3**	**G1**	**G2**	**G3**	**G1**	**G2**	**G3**	**G1**	**G2**	**G3**	**G1**	**G2**	**G3**	**G1**	**G2**	**G3**	**G1**	**G2**	**G3**
White Blood Cell Count	ND	ND	-	ND	ND	-	ND	ND	-	ND	ND	-	ND	ND	-	ND	ND	-	ND	ND	-
Red Blood Cell Count	ND	ND	-	ND	ND	-	5.42	↓4.88	5.42	ND	ND	-	ND	ND	-	ND	ND	-	ND	ND	-
Hemoglobin	ND	ND	-	13.26	↓11.18	13.10	13.84	↓11.80	13.90	12.90	↓11.24	12.75	13.88	↓12.00	14.05	12.42	↓10.36	11.95	13.86	↓11.74	13.10
Hematocrit	ND	ND	-	40.68	34.78	41.30	42.70	↓36.88	45.00	ND	ND	-	ND	ND	-	ND	ND	-	ND	ND	-
MCV	ND	ND	-	ND	ND	-	ND	ND	-	ND	ND	-	ND	ND	-	ND	ND	-	ND	ND	-
MCH	ND	ND	-	ND	ND	-	ND	ND	-	ND	ND	-	ND	ND	-	ND	ND	-	ND	ND	-
MCHC	ND	ND	-	ND	ND	-	ND	ND	-	ND	ND	-	ND	ND	-	ND	ND	-	ND	ND	-
CHCM	ND	ND	-	ND	ND	-	ND	ND	-	ND	ND	-	ND	ND	-	ND	ND	-	ND	ND	-
RDW	ND	ND	-	ND	ND	-	ND	ND	-	ND	ND	-	ND	ND	-	ND	ND	-	ND	ND	-
Platelet Count	305.0	↑424.4	293.5	ND	ND	-	ND	ND	-	ND	ND	-	ND	ND	-	ND	ND	-	ND	ND	-
MPV	ND	ND	-	ND	ND	-	ND	ND	-	ND	ND	-	ND	ND	-	ND	ND	-	ND	ND	-
%NEUT	ND	ND	-	ND	ND	-	ND	ND	-	ND	ND	-	ND	ND	-	ND	ND	-	ND	ND	-
%LYMPH	ND	ND	-	ND	ND	-	ND	ND	-	ND	ND	-	ND	ND	-	ND	ND	-	ND	ND	-
%MONO	ND	ND	-	ND	ND	-	ND	ND	-	ND	ND	-	ND	ND	-	ND	ND	-	ND	ND	-
%EOS	ND	ND	-	ND	ND	-	ND	ND	-	ND	ND	-	ND	ND	-	ND	ND	-	ND	ND	-
%BASO	0.12	↑ 0.22	0.10	ND	ND	-	ND	ND	-	ND	ND	-	↓ 1.06	1.14	2.05	ND	ND	-	ND	ND	-
%LUC	ND	ND	-	ND	ND	-	ND	ND	-	ND	ND	-	ND	ND	-	ND	ND	-	ND	ND	-
#NEUT	ND	ND	-	ND	ND	-	ND	ND	-	ND	ND	-	ND	ND	-	ND	ND	-	ND	ND	-
#LYMPH	ND	ND	-	ND	ND	-	ND	ND	-	ND	ND	-	ND	ND	-	ND	ND	-	ND	ND	-
#MONO	ND	ND	-	ND	ND	-	ND	ND	-	ND	ND	-	ND	ND	-	ND	ND	-	ND	ND	-
#EOS	ND	ND	-	ND	ND	-	ND	ND	-	ND	ND	-	ND	ND	-	ND	ND	-	ND	ND	-
#BASO	ND	ND	-	ND	ND	-	ND	ND	-	ND	ND	-	ND	ND	-	ND	ND	-	ND	ND	-
#LUC	ND	ND	-	ND	ND	-	ND	ND	-	ND	ND	-	ND	ND	-	ND	ND	-	ND	ND	-
Neut%/Lymph% Ratio	ND	ND	-	ND	ND	-	ND	ND	-	ND	ND	-	ND	ND	-	ND	ND	-	ND	ND	-
Neut#/Lymph# Ratio	ND	ND	-	ND	ND	-	ND	ND	-	ND	ND	-	ND	ND	-	ND	ND	-	ND	ND	-

ND= Difference between placebo control and hAd5 S-Fusion + N-ETSD vaccinated NHP for this time point was not statistically significant
↑= increase was statistically significant ($p < 0.05$)
↓= decrease was statistically significant ($p < 0.05$)

Clinical Chemistry

Only creatinine was consistently lower in Group 1 NHP on five time points and at two time points for Group 2 (Table S2), but it was lower on Day 0 baseline, indicating this was not vaccine-related. Data in Table S3

Table S2. *Clinical chemistry for hAd5 S-Fusion + N-ETSD vaccinated Group 1 and Group 2 NHP as compared to placebo Group 3.* ND – not significantly different from placebo. Statistical analyses performed using One-way ANOVA.

Study Day	Day 0			Day 14			Day 28			Day 42			Day 56			Day 63			Day 70		
Parameter	**G1**	**G2**	**G3**	**G1**	**G2**	**G3**	**G1**	**G2**	**G3**	**G1**	**G2**	**G3**	**G1**	**G2**	**G3**	**G1**	**G2**	**G3**	**G1**	**G2**	**G3**
Glucose	ND	ND	-	ND	ND	-	ND	ND	-	ND	ND	-	ND	ND	-	ND	ND	-	ND	ND	-
Blood Urea Nitrogen	ND	ND	-	ND	ND	-	ND	ND	-	ND	ND	-	ND	ND	-	ND	ND	-	ND	ND	-
Creatinine	↓0.57	0.66	0.79	↓0.49	0.58	0.75	↓0.69	0.76	0.88	↓0.59	↓0.64	0.82	↓0.67	↓0.71	0.88	ND	ND	-	ND	ND	-
BUN/Creatinine Ratio	ND	ND	-	32.74	↑42.98	27.15	ND	ND	-	ND	ND	-	ND	ND	-	ND	ND	-	ND	ND	-
Sodium	ND	ND	-	ND	ND	-	ND	ND	-	ND	ND	-	ND	ND	-	ND	ND	-	ND	ND	-
Potassium	ND	ND		ND	ND	-	ND	ND	-	ND	ND	-	ND	ND	-	ND	ND	-	ND	ND	-
Chloride	ND	ND	-	ND	ND	-	ND	ND	-	ND	ND	-	ND	ND	-	ND	ND	-	ND	ND	-
Calcium	ND	ND	-	9.50	↓9.17	9.78	ND	ND	-	ND	ND	-	ND	ND	-	ND	ND	-	ND	ND	-
Phosphorus	ND	ND	-	ND	ND	-	ND	ND	-	ND	ND	-	ND	ND	-	ND	ND	-	ND	ND	-
Total Bilirubin	ND	ND	-	ND	ND	-	ND	ND	-	ND	ND	-	ND	ND	-	ND	ND	-	ND	ND	-
Total Protein	ND	ND	-	ND	ND	-	ND	ND	-	ND	ND	-	ND	ND	-	ND	ND	-	ND	ND	-
Albumin	ND	ND	-	4.40	↓4.00	4.67	ND	ND	-	ND	ND	-	ND	ND	-	ND	ND	-	ND	ND	-
Globulin	ND	ND	-	ND	ND	-	ND	ND	-	ND	ND	-	ND	ND	-	ND	ND	-	ND	ND	-
A/G Ration	ND	ND	-	ND	ND	-	ND	ND	-	ND	ND	-	ND	ND	-	ND	ND	-	ND	ND	-
Alanine Aminotransferase	50.42	↓31.60	55.60	ND	ND	-	ND	ND	-	ND	ND	-	ND	ND	-	ND	ND	-	ND	ND	-
Aspartate Aminotransferase	ND	ND	-	ND	ND	-	ND	ND	-	ND	ND	-	ND	ND	-	ND	ND	-	ND	ND	-
Alkaline Phosphatase	ND	ND	-	ND	ND	-	ND	ND	-	ND	ND	-	ND	ND	-	ND	ND	-	ND	ND	-
Lactate Dehydrogenase	ND	ND	-	ND	ND	-	ND	ND	-	ND	ND	-	ND	ND	-	ND	ND	-	ND	ND	-
Gamma Glutamyl Transferase	ND	ND	-	ND	ND	-	ND	ND	-	ND	ND	-	ND	ND	-	ND	ND	-	ND	ND	-
Sorbitol Dehydrogenase	ND	ND	-	ND	ND	-	ND	ND	-	ND	ND	-	ND	ND	-	ND	ND	-	ND	ND	-
C-Reactive Protein	ND	ND	-	ND	ND	-	ND	ND	-	ND	ND	-	ND	ND	-	ND	ND	-	ND	ND	-

ND= Difference between placebo control and hAd5 S-Fusion + N-ETSD vaccinate NHP for this time point was not statistically significant
↑= increase was statistically significant ($p < 0.05$)
↓= decrease was statistically significant ($p < 0.05$)

Viral gRNA in nasal swab samples

Viral load was determined in nasal swab samples by RT qPCR of genomic RNA. The data for individual NHP at time point post-challenge are shown in Table S3.

Table S3. *Gene copies per mL for gRNA as determined by RT qPCR in nasal passages for all groups.* Values below the level of detection (LOD) of 54 gene copies per mL (GC/mL) are highlighted in yellow. For calculation of the geometric mean, half the LOD values (27 GC/mL) was used.

Animal ID	Grp #	Routes	Sex	Day 56	Day 57	Day 58	Day 59	Day 60	Day 61	Day 62	Day 63	Day 70
RA3938	1	SC-SC-Oral	Male	<LOD	5.47E+08	3.67E+06	2.52E+04	2.50E+04	2.90E+03	1.87E+02	1.04E+03	<LOD
RA3946	1	SC-SC-Oral	Male	<LOD	2.59E+08	2.04E+07	1.38E+06	2.46E+05	9.01E+04	3.29E+03	<LOD	<LOD
RA3945	1	SC-SC-Oral	Male	<LOD	2.06E+07	1.19E+07	9.32E+05	1.73E+05	1.97E+03	9.83E+03	5.71E+02	4.29E+02
RA4002	1	SC-SC-Oral	Female	<LOD	3.84E+07	1.21E+07	5.80E+03	1.95E+05	9.95E+03	<LOD	<LOD	<LOD
RA4000	1	SC-SC-Oral	Female	<LOD	1.52E+10	1.66E+04	2.75E+06	9.18E+05	7.36E+04	1.53E+04	<LOD	7.79E+01
RA3936	2	SC-Oral-Oral	Male	<LOD	1.13E+08	5.06E+06	2.53E+06	5.02E+05	2.04E+03	1.50E+03	<LOD	<LOD
RA3942	2	SC-Oral-Oral	Male	<LOD	3.13E+08	3.59E+06	8.15E+05	5.62E+03	3.32E+02	<LOD	1.01E+02	<LOD
RA3999	2	SC-Oral-Oral	Female	<LOD	1.80E+08	2.65E+07	1.14E+06	3.31E+04	2.39E+03	1.41E+03	1.76E+02	<LOD
RA4014	2	SC-Oral-Oral	Female	<LOD	1.18E+09	4.64E+07	2.69E+05	3.09E+04	1.59E+03	1.68E+03	1.18E+02	<LOD
RA4001	2	SC-Oral-Oral	Female	<LOD	1.67E+07	4.87E+06	3.89E+05	3.95E+04	5.48E+03	1.90E+03	<LOD	2.74E+02
RA3949	3	SC-Oral-Oral	Male	<LOD	2.06E+09	4.95E+08	4.12E+06	7.14E+07	7.02E+05	2.73E+05	1.62E+04	1.74E+04
RA4011	3	SC-Oral-Oral	Female	<LOD	6.95E+07	2.38E+07	3.00E+07	3.44E+05	1.56E+05	7.19E+05	4.61E+05	1.47E+04

Viral gRNA in bronchoalveolar lavage (BAL) samples

Viral load was also determined in BAL samples. Gene copies per mL for individual NHP are shown in Table S4.

Table S4. *Gene copies per mL for gRNA as determined by RT qPCR in BAL samples for all groups.* Values below the level of detection (LOD) of 54 gene copies per mL (GC/mL) are highlighted in yellow. For calculation of the geometric mean, half the LOD values (27 GC/mL) was used.

Animal ID	Group	Routes	Sex	Day 42	Day 57	Day 59	Day 61	Day 63
RA3938	1	SC-SC-Oral	Male	<LOD	1.02E+06	1.26E+05	<LOD	5.24E+02
RA3946	1	SC-SC-Oral	Male	<LOD	1.25E+05	1.04E+05	5.43E+04	3.31E+02
RA3945	1	SC-SC-Oral	Male	<LOD	1.33E+05	7.50E+04	1.22E+05	3.54E+03
RA4002	1	SC-SC-Oral	Female	<LOD	1.40E+06	1.59E+04	8.74E+03	1.55E+02
RA4000	1	SC-SC-Oral	Female	<LOD	1.44E+05	5.00E+03	<LOD	<LOD
RA3936	2	SC-Oral-Oral	Male	<LOD	1.42E+06	3.55E+04	8.53E+03	1.43E+02
RA3942	2	SC-Oral-Oral	Male	<LOD	4.80E+04	1.40E+02	<LOD	1.75E+02
RA3999	2	SC-Oral-Oral	Female	<LOD	3.00E+06	2.28E+06	1.06E+06	1.31E+02
RA4014	2	SC-Oral-Oral	Female	<LOD	2.41E+06	7.39E+05	2.97E+04	1.90E+02
RA4001	2	SC-Oral-Oral	Female	<LOD	6.64E+03	<LOD	<LOD	<LOD
RA3949	3	SC-Oral-Oral	Male	<LOD	6.11E+07	3.44E+06	1.16E+05	2.35E+04
RA4011	3	SC-Oral-Oral	Female	<LOD	1.05E+07	1.20E+06	3.36E+05	1.74E+04

Viral sgRNA in nasal swab samples

Gene copies per mL of subgenomic RNA (sgRNA) for individual NHP are shown in **Table S5.**

Table S5. *Data for sgRNA in nasal swab samples as determined by RT qPCR passages for all groups.* Values below the level of detection (LOD) of 119 gene copies per mL (GC/mL) are highlighted in yellow. For calculation of the geometric mean, half the LOD values (59 GC/mL) was used.

Animal ID	Group	Routes	Sex	Day 56	Day 57	Day 58	Day 59	Day 60	Day 61	Day 62	Day 63	Day 70
RA3938	1	SC-SC-Oral	Male	<LOD	1.12E+07	1.27E+05	<LOD	3.03E+02	<LOD	<LOD	<LOD	<LOD
RA3946	1	SC-SC-Oral	Male	<LOD	1.87E+07	1.21E+06	1.49E+05	1.32E+04	1.64E+04	<LOD	<LOD	<LOD
RA3945	1	SC-SC-Oral	Male	<LOD	1.81E+06	6.41E+05	6.41E+04	1.35E+04	<LOD	1.07E+03	<LOD	<LOD
RA4002	1	SC-SC-Oral	Female	<LOD	3.55E+06	6.65E+05	<LOD	1.45E+04	<LOD	<LOD	<LOD	<LOD
RA4000	1	SC-SC-Oral	Female	<LOD	2.73E+08	4.27E+03	2.38E+05	6.19E+04	<LOD	<LOD	<LOD	<LOD
RA3936	2	SC-Oral-Oral	Male	<LOD	6.57E+06	4.43E+05	1.71E+05	2.52E+04	<LOD	<LOD	<LOD	<LOD
RA3942	2	SC-Oral-Oral	Male	<LOD	1.58E+07	3.43E+05	1.12E+03	<LOD	<LOD	<LOD	<LOD	<LOD
RA3999	2	SC-Oral-Oral	Female	<LOD	1.81E+07	1.99E+06	1.16E+05	1.90E+03	<LOD	<LOD	<LOD	<LOD
RA4014	2	SC-Oral-Oral	Female	<LOD	3.33E+07	2.32E+06	3.26E+04	<LOD	<LOD	<LOD	<LOD	<LOD
RA4001	2	SC-Oral-Oral	Female	<LOD	1.42E+06	4.97E+05	3.84E+04	5.98E+02	<LOD	<LOD	<LOD	<LOD
RA3949	3	SC-Oral-Oral	Male	<LOD	1.33E+08	1.84E+07	3.21E+05	1.49E+06	1.23E+04	2.73E+03	2.86E+02	<LOD
RA4011	3	SC-Oral-Oral	Female	<LOD	4.47E+06	3.81E+06	2.48E+06	5.88E+04	4.40E+04	2.04E+05	1.56E+05	<LOD

813 *Viral sgRNA in BAL samples*
814
815 Gene copies per mL of subgenomic RNA (sgRNA) for individual NHP are shown in Table
816 S5.
817
818 **Table S6.** *Data for sgRNA in BAL samples as determined by RT qPCR passages for all groups.*
819 Values below the level of detection (LOD) of 119 gene copies per mL (GC/mL) are highlighted in
820 yellow. For calculation of the geometric mean, half the LOD values (59 GC/mL) was used.

Animal ID	Group	Routes	Sex	Day 42	Day 57	Day 59	Day 61	Day 63
RA3938	1	SC-SC-Oral	Male	<LOD	9.84E+04	3.48E+04	<LOD	2.58E+02
RA3946	1	SC-SC-Oral	Male	<LOD	2.06E+04	1.12E+04	4.57E+03	<LOD
RA3945	1	SC-SC-Oral	Male	<LOD	1.58E+04	1.32E+04	1.94E+04	<LOD
RA4002	1	SC-SC-Oral	Female	<LOD	1.04E+05	3.11E+03	6.03E+03	<LOD
RA4000	1	SC-SC-Oral	Female	<LOD	9.63E+03	<LOD	<LOD	<LOD
RA3936	2	SC-Oral-Oral	Male	<LOD	1.56E+05	1.11E+04	1.31E+03	<LOD
RA3942	2	SC-Oral-Oral	Male	<LOD	8.88E+03	5.65E+02	<LOD	<LOD
RA3999	2	SC-Oral-Oral	Female	<LOD	2.81E+05	1.38E+05	1.47E+05	<LOD
RA4014	2	SC-Oral-Oral	Female	<LOD	2.74E+05	1.19E+05	1.24E+04	<LOD
RA4001	2	SC-Oral-Oral	Female	<LOD	1.32E+03	<LOD	<LOD	<LOD
RA3949	3	SC-Oral-Oral	Male	<LOD	1.91E+06	5.05E+05	1.57E+04	5.12E+03
RA4011	3	SC-Oral-Oral	Female	<LOD	6.78E+05	9.89E+04	8.58E+03	5.67E+03

821